Analysis of Type II radio burst relationship with CME driven shocks

[*]Raveesha K.H[1], Vedavathi P[2], Vijayakumar H Doddamani[3]
[1] Department of Physics, CMR Institute of Technology, Bangalore -560037, India
[2,3] Department of Physics, Bangalore university,Bengaluru-560056, India

Email : hod.physics@cmrit.ac.in

Abstract- Type II radio bursts are known to be the signatures of coronal shocks. In this paper we examine the relationship between 129 type II bursts in the frequency range 35 – 450 MHz observed at Culgooora observatory during May 2002 – October 2015 and the associated CMEs. We apply Newkirk (1961) density model to determine the formation height of type IIs. We find that in 109/129 cases, type II bursts were preceded/ succeeded by CMEs. The CME associated type II events in which the CME height is above the type II burst source are categorized as group I events (91/129 cases). 91% of the bursts in this group are also associated with flares and 58% of these bursts originate during decaying phase of the flare. The correlation between CME speed and type II shock speed for limb events in this group is 0.33.The CME associated type IIs in which the CME height is below the type II source are categorized as group II (18/129 cases). CME driven shock could have been the exciter of these type II bursts.88% of this group events are associated with flares and 62% of these bursts originate during the rising phase of the flare. The correlation between CME speed and type II shock speed for limb events in this group is 0.96. In 20/129 cases of our data set, type II bursts are not associated with CME and are categorized as group III. 90% of the bursts in this group are associated with flares. 77% of the bursts in the group are originating in the decaying phase of flares. Poor temporal association (9/69 cases) between type IIs and flares of X class during this period. Our results suggest that inspite of temporal association with metric type II bursts, majority of the CME driven shocks (84%) are not successful in exciting type II bursts in 35-450 MHz domain. The type II bursts temporally correlated with CMEs and likely to have been excited by CMEs (type II height > CME height) are originating during the rising phase of the flares in majority of the events. In case of type II bursts temporally correlated with CMEs supposedly not excited by the CMEs (type II height < CME height) ,majority of them are originating in the decaying phase of flares.

Key words: Coronal Mass Ejection-shock-metric-observatory-flare-impulsive

1. INTRODUCTION

Solar type II radio bursts are known to be the signatures of magneto hydrodynamic (MHD) shocks propagating through the solar atmosphere. They are observed as slow drifting emission bands fundamental (F) and harmonic (H) with a frequency ratio of ≈1:2. The frequency drift from high to low frequencies (typically 0.5 MHz/s) is a measure of the decrease of electron density (N_e) with radial distance r in the solar atmosphere. The observed drift rate can be utilized to find velocity if the dependence of N_e on r is known. The characteristics description of solar type II bursts can be found in Nelson & Melrose (1985), Mann et al. (1995), Aurass (1997), and Gopalswamy (2006). MHD shocks in the lower corona ($1\text{-}2R_o$) have been attributed to either solar flares or coronal mass ejections (CMEs) or combination of the two (Gopalswamy 2006; Mann & Vrˇsnak 2007; Pick & Vilmer 2008; Vrˇsnak & Cliver 2008; Nindos et al. 2008). CMEs occurring at the solar limb can be seen in coronagraph images than those near the center of the solar disk (Cliver et al. 1999; Gopalswamy et al. 2001).

Results obtained using radio spectral observations of metric type II bursts indicate that they can be excited by CME driven shocks shocks (Lara et al. 2003; Cliver et al. 2004; Cho et al. 2005, 2007, 2008, 2011; Subramanian & Ebenezer 2006; Mancuso 2007; Gopalswamy et al. 2009a; Liu et al. 2009).Many of these works were carried out without positional information on the type II bursts. Radio heliograph data carry positional information of the type II bursts. Hence the spatial relationship with CMEs and flares can be verified using them. Type II bursts with positional information have been reported by authors (Dulk 1970; Stewart et al. 1974a, 1974b; Nelson & Robinson 1975; Kosugi 1976; Wagner & MacQueen 1983; Gergely et al. 1983; Gary et al. 1984; Gopalswamy & Kundu 1992; Maia et al. 2000; Magdaleni´c et al. 2010; Ramesh et al. 2010; Nindos et al. 2011). These works consisted few selective events.

The relationship between type II bursts and coronal shock waves is established, the physical relationship among metric type II bursts, flares, and coronal mass ejections (CMEs) is not clear. The relationship between metric type II bursts and CMEs is debatable question (Cliver et al. 2004; Vršnak & Cliver 2008; Prakash et al. 2010), whereas for type II bursts at decameter and longer wavelengths there is a consensus that they are driven by CMEs (Cane et al. 1987; Gopalswamy et al. 2000). According to Vrsnak and Cliver (2008) the source of the coronal wave is clear in some events with starting frequencies well below 100 MHz, where the CME is accompanied by a weak flare. They observed that for Moreton-wave-associated type II bursts at higher frequencies (>300 MHz for the harmonic emission), both the CME and the flare are observed. In these events, the CME and the flare are tightly related and, particularly during the impulsive phase, motions of the flare plasma take place together with the CME motions, and both phenomena are potential candidates for producing shocks (Vršnak & Cliver 2008; Magdaleni´c et al. 2012).The study of the relationship between type II bursts and CMEs can be improved by observations of propagating brightness fronts in the extreme ultraviolet (EUV), so-called EUV waves (Moses et al. 1997; Thompson et al. 1998).

Shock waves are an ubiquitous phenomenon in astrophysics. They accelerate electrons (Mann & Classen 1995; Miteva & Mann 2007; Schwartz et al. 2011) and ions (Thomsen et al. 1985; Sckopke 1995; Giacalone 2005).In the solar atmosphere, several kinds of shocks, which manifest as wave-like structures in images are implied in the radio dynamic spectra. Type II radio bursts, following the eruption of coronal mass ejections (CMEs), are a kind of plasma emission with a slow frequency drift in the radio dynamic spectrum, and are generally known to be a signature of coronal shocks (Wild 1950; Zheleznyakov 1970). It is known that most of the interplanetary shocks (within 1 AU) are CME-driven (Cane et al. 1987; Reiner et al. 2001a, 2001b). However, the origin of the metric type II radio bursts is still an open question; they can be generated either by CME-driven shocks (Cliver et al. 2004; Liu et al. 2009; Chen 2011; Cho et al. 2013) or by flare-caused blast waves (Leblanc et al. 2001; Magdalenić et al. 2008; Nindos et al. 2011).

Our present work utilizes a comparatively larger data set (129 events) in the frequency range 35MHz to 450 MHz. In this study we estimate the height of the CME driven shock at the onset of the type II radio bursts.129 events are categorized as Group I (91/129) representing events with CME height at the onset of type II is above the Type II formation height, Group II (18/129) indicating events for which CME height is below the type II formation height and group III (20/129) for type II events not temporally associated with CMEs. We assume that coronal shocks producing metric type II radio bursts are driven by CMEs whose formation height is less than that of type IIs. We calculate the CME height at the type II onset by CMEs extrapolated back to the start time of the type II bursts assuming a constant speed of the CMEs. This approximation is reasonable as acceleration effect will be negligible at high velocities. The kinematics of type II shock is determined by adopting suitable coronal density models. In fact, the real density distribution at the lower corona varies with time and location and the observed CME kinematics might be different at the height where the type II bursts occur since the flare impulsive phase is often associated with CME acceleration phase (Bemporad et al.2003; Guhathakurta & Fisher 1998; Parenti et al. 2000; Zhang et al. 2001).

This paper is organized as follows. Data set is provided in Section 2, data analysis and results are presented in Section 3, followed by a conclusion in Section 4.

2. DATA SET

In this work the type II radio data recorded by the Culgoora observatory *(http://www.sws.bom.gov.au/Solar/2/5/1)* for the period May 2002 to October 2015 is referred. The detailed description is available at this site. The CME data provided by Large Angle Spectrometric Coronograph (LASCO; Brueckner et al.1995) CME catalog http : // cdaw.gsfc.nasa.gov / CME _list /index.html; Yashiro et al.2004; Gopalswamy et al.2009b) on board the Solar Wind Heliospheric Observatory (SoHO) is used to examine whether the radio burst is associated with a CME.. CMEs occurring within 20-30 minutes preceding/succeeding type II bursts have been considered and in most of the cases the temporal association is within 15 minutes. We identified all those Type II radio events for which adequate CME data is available. Few type II events with unclear start time/ end time, insufficient data have not been considered. Our final data set consists of 144 type II bursts categorized as Group I, II & III respectively are listed in table 1, 2 & 3. The columns in the table 1, 2 are : (1) type II date (2) start time (3) end time (4) drift rate (5) shock speed (6) associated flare peak time (7) flare location (8) associated CME detected time (9) CME height at type II start (10) type II formation height (11) type II formation height minus CME height. The columns in table 3 are: (1) type II date (2) start time (3) end time (4) drift rate (5) shock speed (6) associated flare peak time (7) flare location (8) type II formation height. The columns in table 4 are similar to the previous table along with X flare details. We use the flare data recorded by the low energy channel (0.5 – 4Å) of the Reuven Ramaty High Energy Solar Spectroscopic Imager (RHESSI; Lin et al.2002). Flares occurring within +/- 20-30 minutes from the onset of type II bursts are considered as associated flares. For most of the events in our data set, flares/CMEs are observed within 20 minutes from the type II event. Figure 1a shows the dynamic spectrum from Culgoora observatory recorded on 17/05/2012. The frequency range of the spectrometer is from 1800MHz to 18MHz. The fundamental type II burst started from about 40MHz at 01:32 and drifted to 18MHz at 01:40. The mean frequency drift rate of the type II is about 0.20MHz/s close to typical drift rate (~0.3MHz/s) of type IIs reported by Mann (1995). The harmonic band starts at around 80 MHz at 01:32. As seen from the figure 1b, the early eruption of type II associated CME was observed by Large Angle and Spectrometric Coronagraph (LASCO –C2/C3) onboard the Solar and Heliospheric Observatory (SOHO) at 01:48. The first appearance of the CME was at $3.63R_o$ above the solar surface. The acceleration of the CME is -51.8km/s^2. The CME height at the onset of Type II

obtained by extrapolation is 1.45R_o and is above the type II formation height 1.14R_o found by applying Newkirk (1961) density model. This CME is likely to have not excited the type II shown in figure 1a. Figure 1c shows the height –time plot of the leading edge of CME from 01:20 to 04:40.

Figure 1d shows RHESSI X ray flux in the 6-12keV, 12-25keV channels. The associated flare commences at 00:23 reaches the peak at 01:48 close to the type II burst onset time 01:32. In addition, figure 1e shows an M class flare observed by the Geostationary Operational Environmental Satellite (GOES) with onset at 00:28.

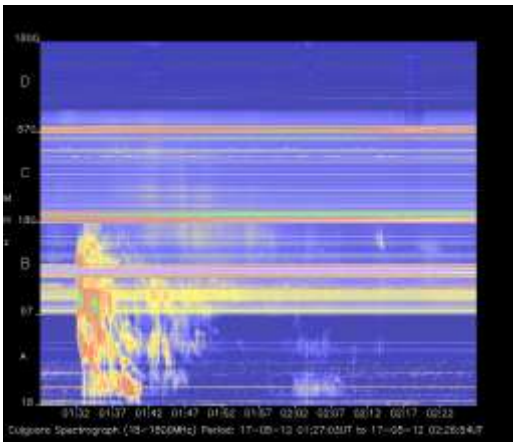

(a)

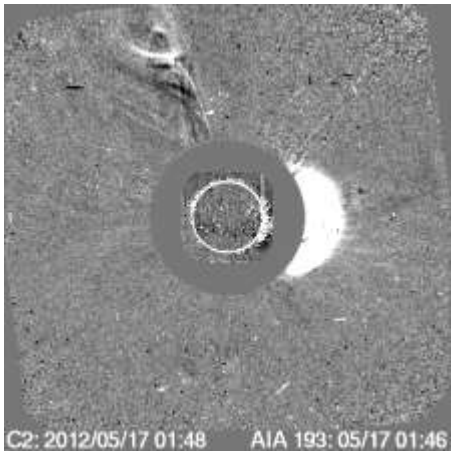

(b)

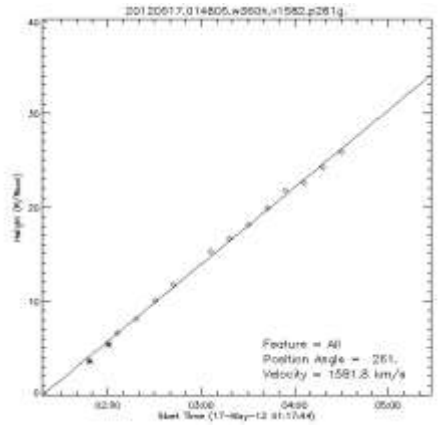

(c) .

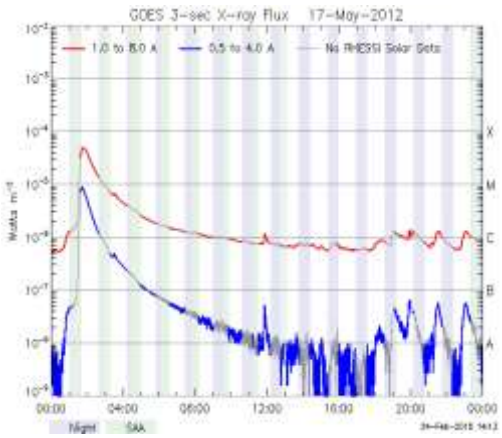

(d)

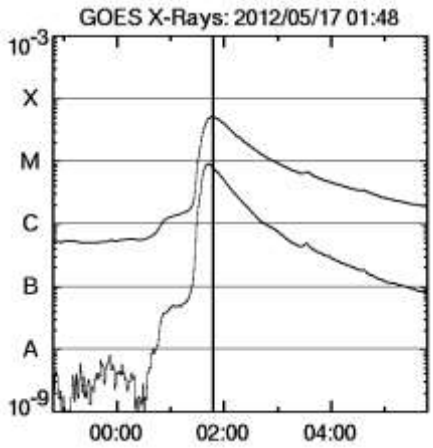

(e)

Figure 1.

(a) Dynamic spectrum of the type II radio burst observed by Culgoora observatory from 01:32-01:40 on 17/5/2012. The burst commences at 40MHz and drifts to 18MHz.Weak band splitting is observed.

(b) The type II associated CME observed by LASCO on 17/5/2012 detected at 01:48 at 3.61R_o occurring 13 minutes after the onset of type II burst.

(c) Height –time plot of the leading edge of CME from 01:20 to 04:40

(d) The type II associated C class flare observed by RHESSI. The flare commences at 00:13:02 (16 minutes before the onset of type II burst) and reaches peak at 01:41 before decaying at 07:26.X ray spectrum at 1-8Å and 0.5-4 Å are shown.

(e) M class flare observed by the Geostationary Operational Environmental Satellite (GOES) with onset at 00:28.The peak time is 01:48 in agreement with RHESSI records.

3. DATA ANALYSIS AND RESULTS

3.1 Type II - CME height relationship

The starting frequencies of type II bursts represent the heights of the radio sources: a higher starting frequency indicates a radio source closer to the solar surface because the frequency of the type II emission is proportional to the square root of the plasma density and the plasma density decreases as a function of radial distance. Most of the density models may differ significantly from the real case and affect the height calculation. In previous studies, the most commonly used density models are Newkirk (1961) and Saito et al. (1977). Since the use of Newkirk (1961) density model to estimate the radio source speed is compatible with radial shock motion [58], we have used Newkirk (1961) density model to determine the formation of height of type II bursts. The Newkirk (1961) density model is given by

$N_e = 4.2x10^4 \times 10^{4.32(Ro/R)}\ cm^{-3}$ where R is the heliocentric distance and R_o is the solar radius.

The CME height at the onset of type II is calculated by back extrapolation assuming constant speed of CMEs.

CME height (at the onset of type II) = CME first appearance height +/- V_{CME} * dt

Here dt is the start time difference between type II & CME.

Table 1 provides details of 91 group I events (type II height – CME height is negative) .It is observed that the type II formation height is in the range of $1.005R_o$ to $1.36R_o$ for more than 83% of the events with an average of $1.16R_o$ close to the results of Cunha-Silva et al.(2015). The average start and end frequency are 201.8 MHz and 39.5MHz respectively with an average bandwidth of 163.34MHz.The average drift rate is 0.24MHz/s close to the typical drift rate (~0.3MHz/s) of type IIs reported by Mann et al.(1995). The average shock speed is 776km/s and the average duration is 10.7minutes.

The CMEs observed in association with these 91 type II events are at heights above the type II formation heights (average height $3.59R_o$). The average width and central position angle of these CMEs is 101.6 deg and 203.5deg.The average speed of these CMEs is 695km/s greater than typical speed of CMEs (450km/s). 65% of CMEs showed deceleration in this group with an average of -5km/s^2. 27% of them are halo CMEs. Poor correlation (0.33) is observed between CME speed and type II shock speed for limb events supporting the argument that blast waves from flares could have excited these type IIs.

Flares are associated in 91% of the events and 58% of these bursts originate during decaying phase of the flare. The drift rates of type IIs associated with different classes of flares are studied for limb events (20/91) in this group. The average drift rate for type IIs accompanying X, C and M class flares in this category is 0.27MHz/s, 0.22MHz/s and 0.17MHz/s respectively. Higher drift rate for bursts associated with X class flares is possibly due to their higher energy. This probably leads to higher shock speed and corresponding higher Alfven speed. This possibly could be one of causes for the absence of association between Type II and X class flares. It may also be noted that drift rate corresponds to energy associated with the respective class of the flare.

Table 2 provides the details of 18 group II events (type II height – CME height is positive). It is observed that the type II formation height is in the range of $1.07R_o$ to $1.29R_o$ for more than 55% of the events with an average of $1.19R_o$.The average start and end frequency are 194.8 MHz and 36.3MHz respectively with an average bandwidth of 158.5MHz.The average drift rate is 0.20MHz/s slightly less than the typical drift rate (~0.3MHz/s) of type IIs reported by Mann et al. (1995). The average shock speed is 745km/s and the average duration is 11.14minutes.

The CMEs observed in association with these 18 type II events are originating at a height lower than the type II formation heights (avg ht $1.19R_o$). The average width and central position angle of these CMEs is 162 deg and 211.8 deg. The average speed of these CMEs is 1101 km/s which is almost 3 times greater than typical speed of CMEs (450km/s). 74% of CMEs showed deceleration in this group with an average of -15km/s^2. 44% of them are halo CMEs. The strong correlation (0.96) between CME speed and type II shock speed for limb events is noticed. This supports the view that these type IIs could have been excited by CME driven shocks.

Flares are associated in 88% of these events. Unlike group I events, 62% of these bursts originate during the rising phase of the flare. Average drift rate for type IIs accompanying C and M class flares in this category is 0.16MHz/s, 0.20MHz/s respectively.

The details of group III type II events not associated with CMEs are given in table 3. It is observed that the type II formation height is in the range of $1.11R_o$ to $1.29R_o$ for more than 63% of the events with an average of 1.24Ro.The average start frequency is 138 MHz significantly lesser than group I and II events. The average drift rate is 0.26MHz/s .The average shock speed is 645km/s which is lesser than the group 1 & 2 bursts. The average duration is 8.16minutes. Flares are present in 90% of the events in this group. 77% of these bursts are originating in the decaying phase of the flare. Average drift rate for type IIs accompanying C and M class flares in this category is 0.39MHz/s, 0.31MHz/s respectively.

We repeated these calculations by applying Saito's density model (Saito et al, 1977) of the form

$n(r) = 10^8 \times (0.0136r^{-2.14} + 1.68r^{-6.13})$

with a multiplication factor of 10 and obtained almost similar results.

Histograms representing the distribution of type II parameters such as life time, bandwidth, drift rate, start frequency, shock speed and CME parameters such as CME speed, acceleration/ deceleration corresponding to group I and II are shown in figures 2a to 2t.

3.2 Impulsive X class flare events and type II bursts

X class flares release large amount of energy. However type II bursts are not found to be associated with these flares in most of the cases. During the period 2002-2015, 70 Impulsive flares of X class are observed with sufficient data. We identified Type IIs and CMEs accompanying the X class flares. Neglecting events with unclear start/end time, insufficient data, our final data set contains 69 X class flares. These flares display sharp rising phase where as the decaying phase is exponential. The details of these flares and the accompanying type IIs & CMEs are provided in table 4. In 58/69 cases CMEs are temporally associated with flares. In 35/58 cases, the CMEs associated were found to be halo. The speeds of CMEs associated with X class are higher (avg 1259 km/s) than group I and II counterparts in agreement with results of Magdalenic et al.(2010).In 29/69 events, CME speeds are higher than 1000km/s.

It is interesting to note that only in 9/69 cases type IIs are observed. The characteristics of these 9 type IIs are studied. They possess higher drift rate (avg 0.51MHz/s). In most of these cases , the associated CMEs are ahead of type IIs supporting the opinion that high pressure blast waves caused by the flares could have been the exciters of type II bursts. However, the correlation between type II speed and CME speed is 0.56. We find that in 7/9 cases, the type II bursts are originating during rising phase of the flare and their average start frequency, bandwidth and velocity of type II shock waves are significantly higher than group I & II events. It was observed in few cases that type IIs accompanied C class flares rather than X class flares on a day when both the classes of flares were present.

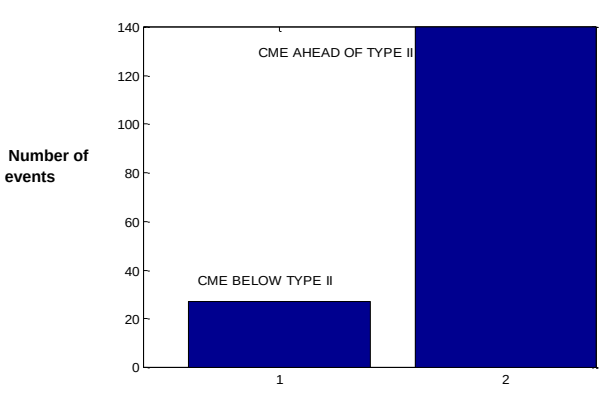

(a)

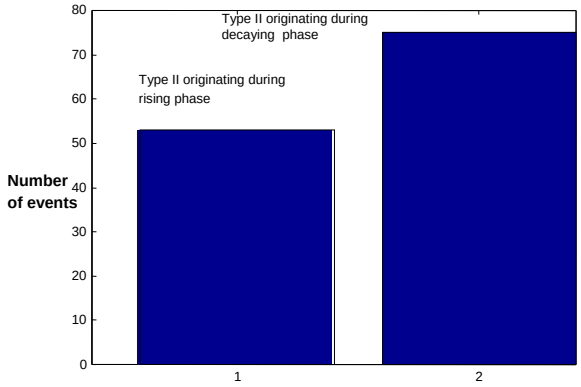

(b)

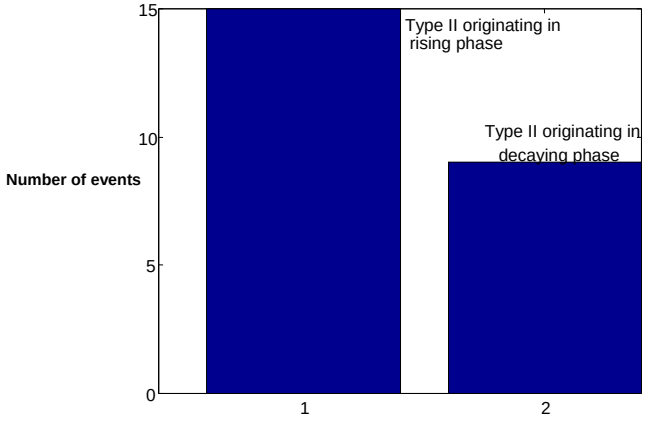

(c)

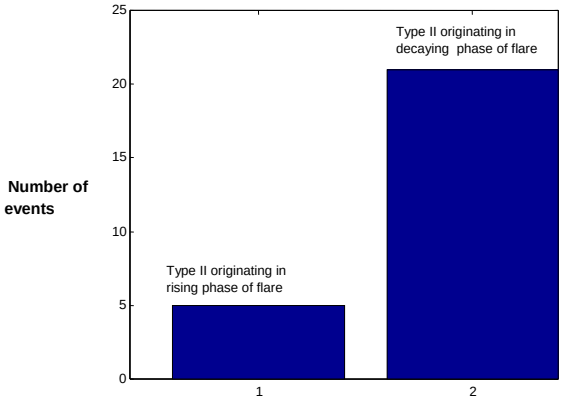

(d)

GROUP I (Type II height > CME height)

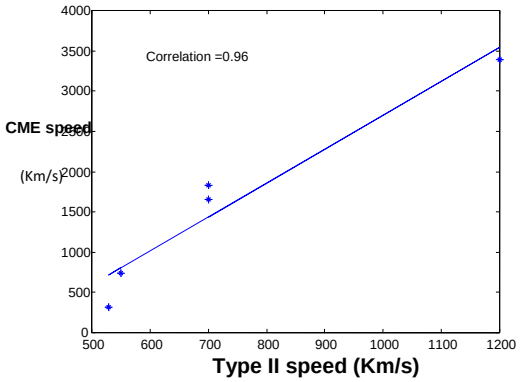

(e)

GROUP I (Type II height > CME height)

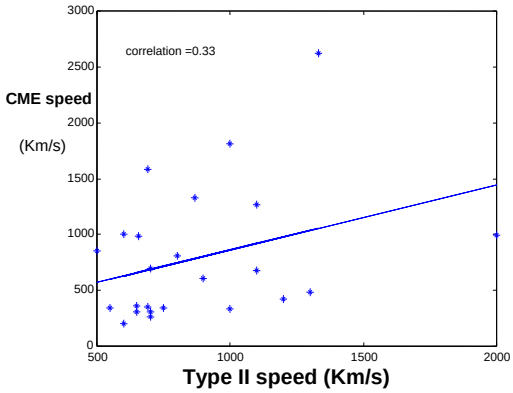

(f)

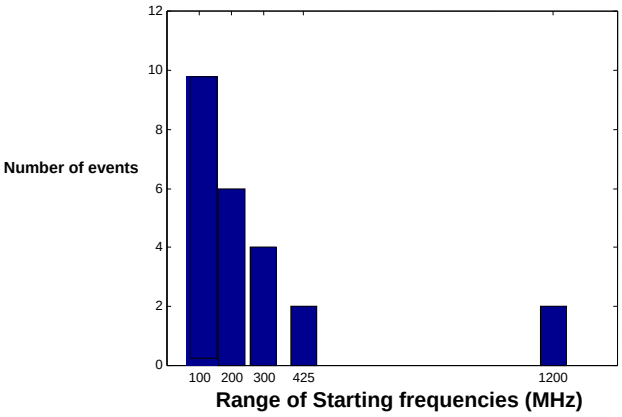

(g)

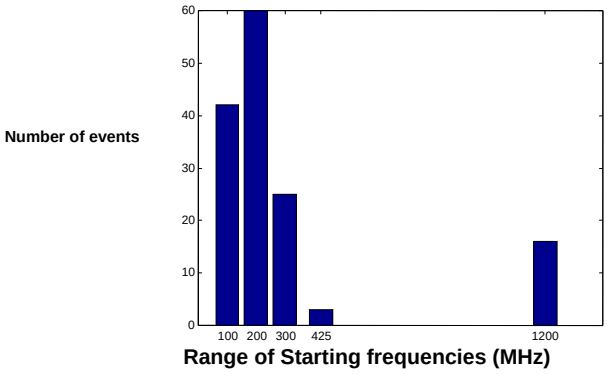

(h)

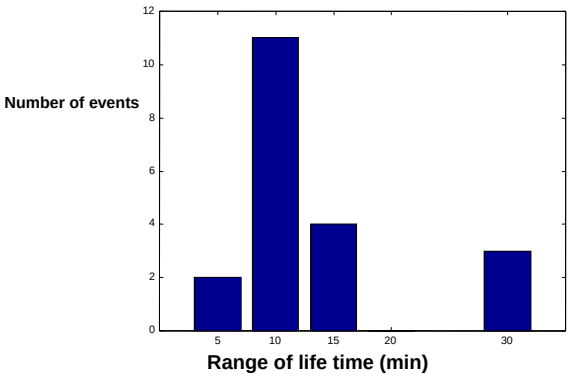

(i)

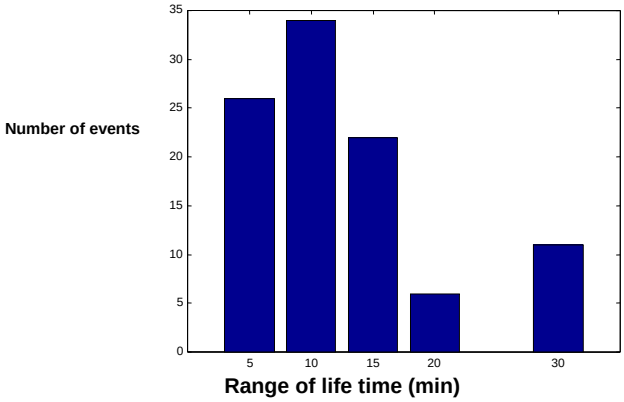

(j)

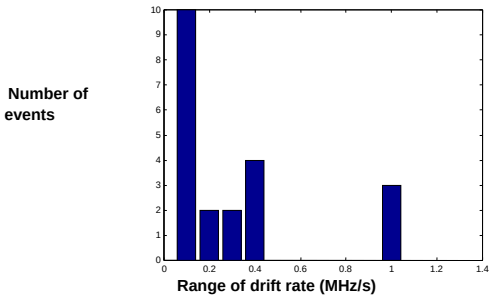

(k)

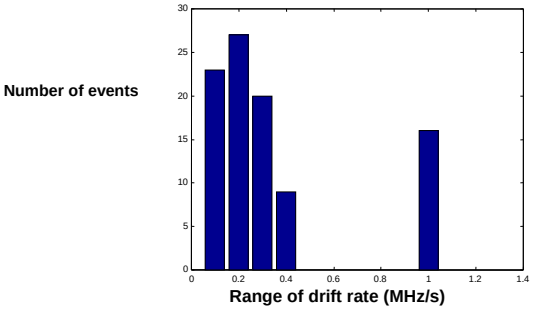

(l)

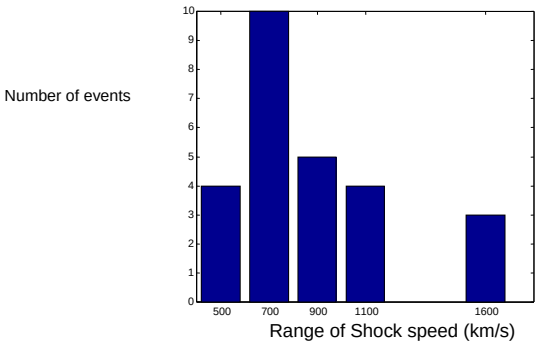

(m)

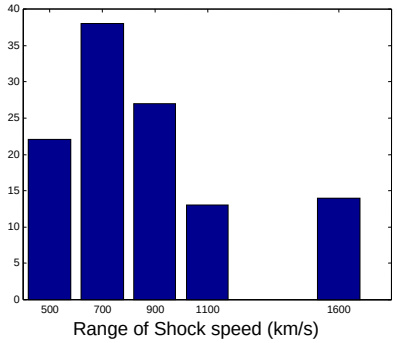

(n)

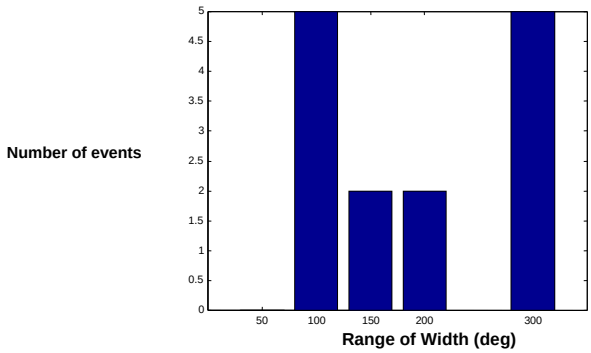

(o)

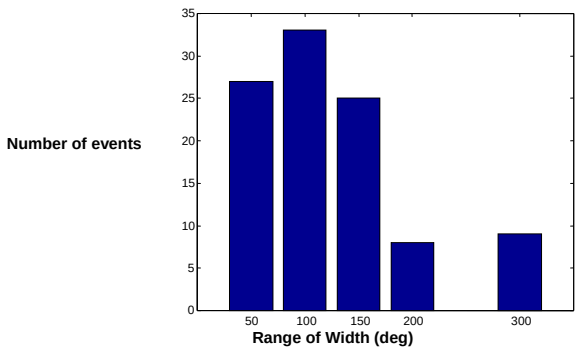

(p)

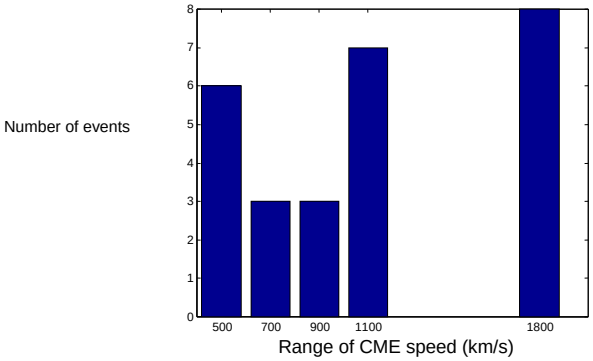

(q)

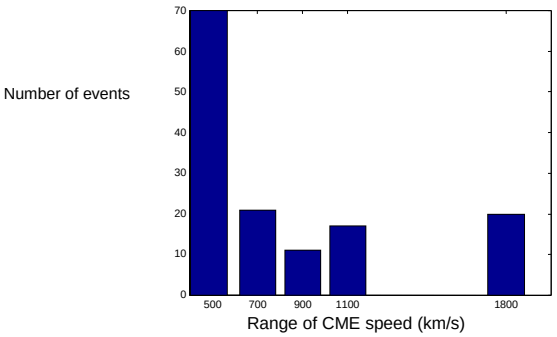

(r)

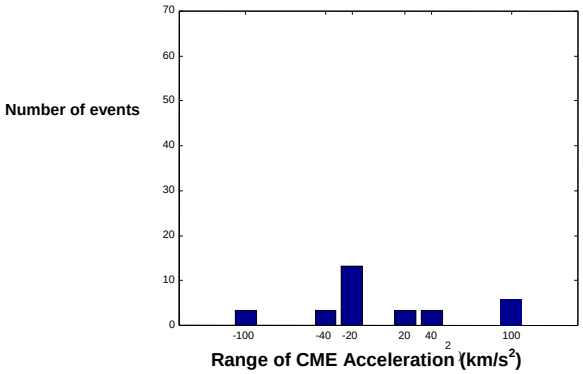

(s)

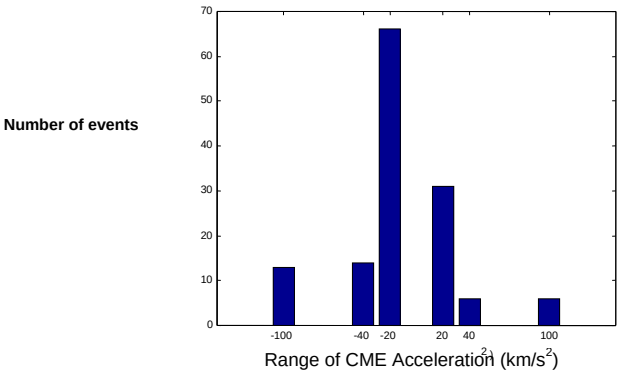

(t)

Figure 2.
a: Distribution of CME based on their height
b: Type II and flare association for group I events
c:Type II and flare association for group II events
d: Type II and flare association for group III events
e: Scatter Plot of CME speed and Type II speed for
f: Scatter Plot of CME speed and Type II speed for Group I

Group II events

g: Distribution of starting frequencies for Group II events h: Distribution of starting frequencies for Group I events
i: Distribution of life time for Group I events j: Distribution of life time for Group II events
k: Distribution of drift rate for Group II events l: Distribution of drift rate for Group I events
m:Distribution of shock speed for Group I events n: Distribution of shock speed for Group II events
o: Distribution of Bandwidth for Group II events p: Distribution of Bandwidth for Group I events
q: Distribution of CME speed for Group II events r: Distribution of CME speed for Group I events
s: Distribution of CME acceleration for group II events t: Distribution of CME acceleration for group II events

Table 1. Type II –Flare – CME parameters for GROUP I events

Date	Type II				Flare		CME	Height (R_o) based on Newkirk model		
	start time (UT)	End time (UT)	Drift rate (MHz/s)	Shock speed (km/s)	peak time(UT)	Location	CME detected time (UT)	CME Height at the start of Type II	Type II start height	Type II -CME height difference
24/5/2002	0322	0328	0.2306	500	-	-	0330	1.95	1.1488	-0.8012
31/05/2002	0304	0314	0.0317		-	-	0326	2.13	1.3375	-0.7925
20/7/2002	2107	2137	0.0911	600	2120	-	2118	6.54	1.0392	-5.5008
14/8/2002	0148	0209	0.0659	400	0207	-	0230	2.08	1.1488	-0.9312
16/8/2002	0522	0554	0.0641	1700	-	-	0530	2.71	1.0858	-1.6242
18/8/2002	2124	2130	0.2306	1000	2150	-	2154	1.577	1.1488	-0.4282
21/8/2002	0154	0200	0.0639	450	0144	-	0131	3.58	1.3193	-2.2607
22/8/2002	0156	0202	0.3417	800	0152	-	0206	2.52	1.0858	-1.4342
24/8/2002	0106	0114	0.2188	773	0113	-	0127	2.46	1.1083	-1.3517
24/8/2002	2051	2052	0.25	718	2030	-	2020	4.797	1.1774	-3.6196
8/9/2002	0152	0157	0.1167	900	-	-	0206	2.06	1.2456	-0.8144
16/9/2002	0316	0321	0.1	750	0349	-	0306	3.37	1.2793	-2.0907
19/9/2002	0521	0524	0.4611	1000	0526	-	0554	1.61	1.1488	-0.4612
19/9/2002	0530	0539	0.0611		-	-	0554	2.09	1.2793	-0.8107
5/10/2002	2057	2118	0.0929	272	2100	-	2154	1.21	1.0858	-0.1242
27/10/2002	2259	2310	0.2152	900	2200	-	2318	3.87	1.1144	-2.7556
19/10/2002	2139	2158	0.1404	850	2152	-	2206	1.68	1.0858	-0.5942
21/1/2003	0227	0234	0.2143	700	0226	N14W00	0254	1.74	1.1688	-0.5712
23/1/2003	0448	0459	0.0894	324	0449	S22E12	0530	1.86	1.2394	-0.6206
12/2/2003	0151	0156	0.4567	700	0146	S06W55	0230	1.32	1.0181	-0.3019
23/4/2003	0102	0107	0.4767	679	0107	N18W32	0127	1.67	1.0731	-0.5969
25/4/2003	0530	0538	0.0667	800	0544	N16E61	0550	1.56	1.4497	-0.1103
26/4/2003	2340	2347	0.3524		2336	N18W71	2326	2.76	1.078	-1.682
29/5/2003	0106	0111	0	800	0102	S07W46	0127	4	2.1831	-1.8169
6/6/2003	2341	2351	0.075	415	2333	N12E09	2354	1.85	1.3237	-0.5263
17/6/2003	2248	2258	0.3	1000	2254	S07E58	2318	2.4	1.0613	-1.3387
17/6/2003	2003	2010	0.1667	1500	1956	-	1954	5.85	1.2793	-4.5707
7/1/2004	0406	0420	0.0726	692	0407	N05E64	0406	3	1.283	-1.717
19/1/2004	2003	2014	0.2197	450	1957	-	1931	3.03	1.0858	-1.9442
20/1/2004	0739	0750	0.2348	550	0741	S14W22	0830	1.42	1.0858	-0.3342
5/4/2004	0554	0606	0.1333	615	0546	S16E25	0506	5.1	1.1774	-3.9226
16/6/2004	0423	0425	0.7917	2000	0433	S10E51	0436	2	1.1912	-0.8088
5/7/2004	2232	2243	0.0848	424	-	-	2306	2.22	1.2906	-0.9294
24/8/2004	2110	2134	0.0535	800	2107	-	2130	3.17	1.2618	-1.9082
31/8/2004	0541	0554	0.0987	650	0533	N03W88	0554	2.09	1.2456	-0.8444
12/9/2004	0142	0148	0.1556	866	0049	S01W72	0036	9.82	1.3025	-8.5175
10/10/2004	2128	2138	0.3283	559	2157	-	2154	1.52	1.0074	-0.5126
30/10/2004	0329	0344	0.0556	800	0326	N14W25	0354	2.65	1.3423	-1.3077
30/10/2004	0613	06331	0.0351	1800	0705	N14W25	0654	1.87	1.3237	-0.5463
15/1/2005	2234	2242	0.1354	1200	2257	N13W03	2306	1.51	1.3065	-0.2035

17/4/2005	0144	0155	0.1182	690	0141	S11E76	0206	1.83	1.196	-0.634
19/4/2005	2150	2202	0.0861	1150	2205	-	2206	1.63	1.2984	-0.3316
2/5/2005	2239	2246	0.0357		2241	-	2226	3.56	1.6899	-1.8701
15/5/2005	2235	2240	0.25	650	2231	S15E16	2326	2.26	1.2456	-1.0144
3/6/2005	0416	0429	0.1538	350	0413	S17E09	0332	3.98	1.1129	-2.8671
3/7/2005	0503	0510	0.3095	900	0502	S11E34	0530	1.61	1.1144	-0.4956
31/12/2007	0054	0058	0.1125		0102	S13E86	0142	2.05	1.3282	-0.7218
18/3/2010	2311	2314	0.4722	550	-	-	2354	1.52	1.1912	-0.3288
25/3/2010	0128	035	0.2381	850		-	0131	3.66	1.1488	-2.5112
12/6/2010	0058	0109	0.1864	1300	0057	N24W58	0131	2.18	1.0858	-1.0942
13/6/2010	0539	0545	0.3417	700	0531	N24W76	0530	3.35	1.0858	-2.2642
12/11/2010	0139	0146	0.3381	500	0133	S22W10	0224	2.585	1.1144	-1.4706
28/1/2011	0102	0111	0.1352	900	0054	N09W69	0125	1.81	1.1688	-0.6412
17/4/2011	2138	2144	0.175	1000	-	-	2236	2.356	1.1912	-1.1648
8/9/2011	2158	2209	0.1212	-	-	-	2212	1.69	1.1688	-0.5212
23/9/2011	2353	2357	0.2833	998	2210	N13E59	2340	3.01	1.1646	-1.8454
2/10/2011	0051	0055	0.1792	299	0044	N12W25	0200	1.13	1.0952	-0.0348
15/11/2011	0012	0016	0.5417	600	0000	-	0012	2.61	1.0858	-1.5242
17/11/2011	0142	0146	0.3333	600	-	-	0200	2.251	1.1912	-1.0598
25/11/2011	2154	2159	0.1967	701	2157	N16W65	2224	1.71	1.2139	-0.4961
17/5/2012	0132	0142	0.2033	1100	0141	-	0148	1.45	1.1488	-0.3012
2/7/2012	0509	0515	0.4167	700	0510	S17E04	06	1.632	1.0731	-0.5589
6/7/2012	2309	2317	0.1375	1357	2302	S18W50	2324	2.68	1.2868	-1.3932
31/7/2012	0001	0010	0.1704	1000	0024	-	0012	2.482	1.2165	-1.2655
3/8/2012	0603	0616	0.0692	506	0601	-	0624	2.102	1.2757	-0.8263
6/8/2012	0443	0000	0.0882	600	0437	S13E75	0512	1.958	1.0858	-0.8722
8/8/2012	0059	0104	0.4	657	0045	N20E76	0048	3.769	1.0719	-2.6971
12/8/2012	2328	2338	0.225	400	2327	S22E43	0054	3.25	1.0995	-2.1505
13/8/2012	0211	0215	0.0583	575	0214	S23E21	0224	2.742	1.536	-1.206
7/10/2012	2120	2123	0.4	1029	2122	-	2136	1.67	1.1646	-0.5054
13/5/2013	0212	0227	0.1067	1100	0212	N12E81	0200	3.896	1.206	-2.69
14/5/2013	0107	0120	0.2628	1330	0124	N11E63	0125	1.79	1.0216	-0.7684
6/7/2013	0156	0205	0.0963	1000	0151	-	02	2.354	1.3678	-0.9862
30/8/2013	0219	0225	0.1111	700	0227	N11E33	0248	1.874	1.4283	-0.4457
11/10/2013	0710	0720	0.3783	924	0715	S27E50	0724	1.21	1.0131	-0.1969
7/11/2013	0341	0347	0.5556	600	0339	-	0424	1.096	1.0051	-0.0909
8/1/2014	0349	0402	0.1923	600	0346	-	0412	1.57	1.0858	-0.4842
17/1/2014	0228	0234	0.1111	500	0222	-	0248	2.02	1.3193	-0.7007
20/2/2014	0322	0333	0.0833	600	0328	S11E32	0322	3.7	1.2793	-2.4207
25/2/2014	0057	0102	0.19	2000	0046	S12E64	0125	8.79	1.3423	-7.4477
28/2/2014	2344	2358	0.031	649	2342	-	2348	2.884	1.3678	-1.5162
17/12/2014	0443	0509	0.0333	600	0442	-	05	2.395	1.3678	-1.0272
20/12/2014	0056	0111	0.0622	850	0043	-	0125	1.95	1.3472	-0.6028
9/2/2015	2314	2326	0.0903	650	2325	N14E51	2324	1.642	1.2793	-0.3627
3/3/2015	0134	0141	0.2857	750	0133	-	0136	2.582	1.0858	-1.4962
11/3/2015	0003	0007	0.4167	700	0001	S16E14	0024	1.64	1.1488	-0.4912
12/3/2015	0220	0225	0.4	500	0200	-	0248	2.01	1.0995	-0.9105
17/3/2015	2332	2342	0.375	600	2330	S21W56	2348	1.92	1.0051	-0.9149
21/4/2015	225	242	0.1284	300	219	-	212	3.05	1.0925	-1.9575
22/7/2015	650	708	0.1241	500	659	S15E20	712	1.92	1.1176	-0.8024

Table 2. Type II –Flare –CME parameters for GROUP II events

	TYPE II				Flare		CME	Height (R_o) based on Newkirk model		
Date	start time (UT)	End time (UT)	Drift rate (MHz/s)	Shock speed (Km/s)	Peak (UT)	Location	CME detected time (UT)	CME Height at the start of Type II	Type II start height	Type II - CME height difference
30/5/2002	2312	2344	0.061	-	-	-	2326	0.9	1.0884	0.1884
23/8/2002	0549	0611	0.093	530	-	-	0625	1.04	1.0858	0.0458

24/11/2002	2006	2016	0.028	800	2019	-	2030	1.53	1.6899	0.1599
27/1/2003	2148	2201	0.038	200	2111	S19W13	2223	0.59	1.4497	0.8597
31/5/2003	0220	0233	0.26	700	0227	S07W72	0230	0.93	1.0059	0.0759
2/6/2003	0019	0026	0.364	700	0015	S07W72	0030	0.99	1.0858	0.0958
1/11/2003	2233	2240	0.3	962	2236	-	2306	0.48	1.1053	0.6253
1/11/2003	0023	0028	0.183	770	0016	-	0054	1.16	1.2984	0.1384
4/11/2004	2222	2228	0.089	550	2230	-	2330	-2	1.3472	3.3472
6/11/2004	0036	0041	0.08	593	0032	-	0131	-0.23	1.3282	1.5582
22/9/2005	0102	0108	0.111	1200	0133	-	0131	0.96	1.4283	0.4683
15/2/2011	0152	0200	0.423	800	0155	S21W27	0224	0.6	1.0051	0.4051
3/7/2011	0004	0006	0.417	1043	0008	N16W38	0048	1.01	1.1936	0.1836
9/9/2011	0615	0619	0.075	529	0609	N17W55	0724	0.73	1.4497	0.7197
6/2/2013	0007	0013	0.347		0004	N22E01	0024	0.82	1.1308	0.3108
20/3/2014	0400	0407	0.064	550	0354	S15E60	0436	0.4	1.4497	1.0497
15/3/2015	0115	0135	0.066	500	0056	S16W26	0148	1.21	1.2112	0.0012
25/8/2015	2217	2228	0.056	500	2215	-	2312	1.22	1.4283	0.2083

Table 3. Type II –Flare parameters for GROUP III events

	Type II				Flare		Type II height (R_o) based on Newkirk model
Date	start time (UT)	End time (UT)	Drift rate (MHz/s)	Shock speed (Km/s)	Peak (UT)	Location	
16/7/2002	2201	2206	0.26	557	2141	-	1.1507
19/7/2002	0331	0333	0.24	325	0246	-	1.1414
25/8/2002	0325	0329	0.23	484	0323	-	1.1053
2/9/2002	0012	0014	0.79	1897	.....	-	1.116
8/9/2002	0156	0203	0.07	500	0136	-	1.2686
30/9/2002	0425	0428	0.11	1000	0420	-	1.4811
14/10/2002	0003	0008	0.31	1000	0005	-	1.1912
31/1/2003	2208	2226	0.07	505	2241	-	1.2086
19/7/2003	0139	0143	0.06	551	0136	N16W20	1.4982
20/1/2004	0748	0757	0.12	850	0741	S14W22	1.2456
27/4/2004	0716	0735	0.14	600	0723	-	1.0731
24/6/2004	0619	0626	0.24	565	0605	S11W53	1.1507
31/8/2004	0547	0554	0.13	400	0536	N03W88	1.2984
18/8/2006	2357	2359	0.75	630	2326	-	1.1488
19/2/2007	0018	0024	0.16	500	0013	S12E04	1.2793
3/3/2011	0343	0350	0.24	900		-	1.1144
30/9/2011	0252	0256	0.07	676	0249	N13W29	1.4352
13/12/2011	0316	0323	0.15	-	-	-	1.1912
15/12/2013	2027	2042	0.09	600	-	-	1.2165
22/6/2015	0600	0607	0.07	325	0518	-	1.2305

Table 4. X class flare – Type II – CME parameters

Date	Flare			Type II			CME	
	peak time (UT)	Location	class	start time(UT)	end time(UT)	drift date(MHz/s)	Detected time (UT)	Speed (Km/s)
27/5/2003	0028	S07 W20	X1.3	2302	2310	0.52	….	
29/5/2003	0057	S07W46	X1	Insufficient data			0127	1237
9/6/2003	2139	N12W32	X1.7	2138	2152	0.392	….	
10/6/2003	0002	N12W36	X1.4				0056	730
15/6/2003	2356	S07E85	X1.3				2354	2053
19/10/2003	1649	N06E53	X1.1				1708	472
23/10/2003	0826	S16E70	X5.4				0854	511

26/10/2003	0639	S06E18	X1.2				0654	1371
28/10/2003	1110	S07E04	X17.2				1054	1054
29/10/2003	2049	S16W11	X10	2042	2050	0.562	2054	2029
2/11/2003	1720	S17W62	X8.3				1730	2598
3/11/2003	0952	N08W82	X3.9				1006	1420
	0128		X12.7				0159	827
4/11/2003	1949	S17W89	X17				1954	2657
26/2/2004	0203	N14W27	X1.1				..	
30/10/2004	1146	N14W25	X1.2				1230	427
7/11/2004	1602	N08W22	X2				1654	1759
10/11/2004	0207	N08W62	X2.5	Insufficient data			0226	3387
1/1/2005	0031	N05E21	X1.7	29	50	0.555	0054	832
15/1/2005	2252	N13W03	X1.2				2306	2861
17/1/2005	0952	N13W30	X3.8				0954	2547
19/1/2005	0818	N14W56	X1.3				0829	2020
20/1/2005	0657	N14W70	X7.1	636	800	0.175	0654	882
14/7/2005	1055	N12W97	X1				….	
30/7/2005	0635	N12E52	X1.3				0650	1968
7/9/2005	0739	S12E83	X17				….	
8/9/2005	2102	S09E67	X5.4				….	
9/9/2005	1952	S09E67	X5.4				1948	257
10/9/2005	2202	S09E44	X1.1				2152	1893
13/9/2005	1927	S11E04	X1.5				2000	1866
15/9/2005	0838	S11W22	X1.1				…	
5/12/2006	1026	S06E72	X9				…	
6/12/2006	1847	S05E60	X6				…	
13/12/2006	0241	S05E33	X3.4				0254	1774
14/12/2006	2215	S05W47	X1.5				2230	1042
9/3/2011	2323	N09W12	X1.5				2305	332
9/8/2011	0754	N17W81	X6.9				0812	1610
6/9/2011	2220	N14W18	X2.1				2305	575
7/9/2011	2238	N14W32	X1.8				2305	792
22/9/2011	1101	N17E76	X1.7				1048	1905
24/9/2011	0940	N12E47	X1.9				0948	1936
3/11/2011	2027	N18E57	X1.9				…	
27/1/2012	1839	N29W88	X1.7				1827	2508
5/3/2012	0409	N17E41	X1.1				0400	1531
7/3/2012	0024	N17E15	X5.4				0024	2684
12/7/2012	1657	S16W09	X1				1648	885
23/10/2012	0317	S12E43	X11	317	321	1.417	….	
13/5/2013	0215	N12E81	X2.8	212	227	0.106	0200	1270
14/5/2013	0113	N11E66	X3.2	107	120	0.262	0125	2625
15/5/2013	0144	N11E66	X1.2	Insufficient data			0148	1366
25/10/2013	0801	S09E63	X1.7				0812	587
28/10/2013	0203	N06W81	X1.0	Insufficient data			0224	695
5/11/2013	2212	S11E38	X3.3	Insufficient data			2236	562

8/11/2013	0426	S10W02	X1.2	424	437	0.856	….
10/11/2013	0514	S11W29	X1.1			0536	682
29/3/2014	1748	N10W36	X1			1812	528
25/4/2014	0024	S14W90	X1.7			0048	456
10/6/2014	1252	S17E82	X1.5			1310	1469
	1142	S15E80	X2.2			1148	924
11/6/2014	0906	X18E65	X1			0924	829
19/10/2014	0503	S13E57	X1.3			0448	139
22/10/2014	1428	S14E13	X1.6			1400	655
24/10/2014	2141	S12W21	X3.1			2148	184
25/10/2014	1708	S16W21	X1			1736	171
26/10/2014	1056	S18W40	X2			…..	
27/10/2014	1447	S17W52	X2			1512	170
7/11/2014	1724	N17E40	X1.6			1712	469
11/3/2015	1622	S17E02	X2.1			1700	240
5/5/2015	2211	N12E70	X2.7			2224	715

4. CONCLUSIONS

In this paper we study the relationship between type II bursts and CMEs. We find that in the metric domain in 70% of the events in our data set, the type II formation height is below the CME height indicating that CMEs are less successful in exciting type II bursts in the metric domain. The main results of the paper are summarized as follows.

1. We apply the Newkirk density model to determine the type II bursts and compare it with CME height at the onset of type II.
2. We classify the events as group I, II & III depending whether type height - CME height is positive, negative or CME is not present respectively. We have found that type II parameters are slightly higher for group I events than group II events. Type II bursts not associated with CMEs possess lesser shock speed, bandwidth and duration. In 83% of type II events, our results suggest that inspite of temporal association, majority of the CME driven shocks are not successful in exciting type II bursts in 35-450 MHz domain.
3. CME parameters are greater for group II events than group I events. This supports the earlier results which indicated that CMEs successful in exciting type II bursts are stronger with greater speed & width.
4. Fairly equal amount of flare association exists in group I, II & III events. Despite poor correlation is observed between type IIs and X class flares, such type IIs possess higher drift rates. Majority of X class flares are accompanied by CMEs which possess higher speed (avg 1259km/s).
5. The type II bursts likely to have been excited by CMEs are originating during the rising phase of the flares in majority of the events and in case of type II bursts supposedly not excited by the CMEs, majority of them are originating in the decaying phase of flares.
6. We applied Saito (1977) density model and obtained similar results.

ACKNOWLEDGEMENTS

We are deeply indebted to authorities of Indian Institute of Astrophysics, Bangalore, CMR Institute of Technology, Bangalore and Bangalore university, Bangalore for the support and encouragement. We are grateful to the authorities of Culgoora observatory, SOHO and RHESSI teams for their open data policy.

REFERENCES

1. Aurass, H., 1997, Coronal Physics from Radio and Space Observations, edited by G. Trottet, Springer, Berlin, p.135, 1997.
2. Bemporad, A., Poletto, G., Suess, S. T., Ko, Y. K., Parenti,S., Piley,P., Romoli, M., & Zurbuchen, T. Z. 2003, ApJ, 593, 1146
3. Brueckner, G. E, et al. 1995, Sol. Phys., 162, 357
4. Cane, H. V., Sheeley, N. R., Jr., and Howard, R. A.: 1987, J. Geophys. Res. 92, 9869.
5. Chen, P.F.: Living Reviews in Solar Physics, Volume 8, Issue 1, article id.1, 92 pp
6. Cho, K.-S., Lee, J., Gary, D. E., Moon, Y.-J., & Park, Y. D. 2007, ApJ, 665,799
7. Cho, K.S., et al. 2011, Astronomy & Astrophysics, Volume 530, id.A16, 5 pp
8. Cho, K.-S., et al. 2005, J. Geophys. Res., 110, A12101
9. Cho, K.-S., et al. 2008, A&A, 491, 873
10. Cho, K.-S.,et al, Lee, J., Gary, D. E., Moon, Y.-J., & Park, Y. D. 2007, ApJ, 665,799
11. Cho, K-.S. ,et al, 2013, Solar Physics, Volume 284, Issue 1, pp.105-127

12. Cliver, E. W., D. F. Webb, and R. A. Howard. 1999. Solar Phys. 187, 89–114.
13. Cliver, E. W., Kahler, S. W., & Reames, D. V. 2004, ApJ, 605, 902
14. Dulk, G. A., 1970, Proceedings of the Astronomical Society of Australia, Vol. 1, p.308
15. Gary et al. 1984, A& A.134, 222
16. Gergely,T.E., et al. 1983; Astrophysical Journal, 268, 403-411.
17. Giacalone,J.:Jokipii,J.R.,2005,American Geophysical Union, Fall Meeting , abstract #SH52A-03
18. Gopalswamy, N. and Kundu, M. R.: 1992, in G. P. Zank and T. K. Gaisser (eds.), AIP Conf. Proc.
19. Gopalswamy & S. Yashiro, 2011,Astrophys. J., 736, L17
20. Gopalswamy, N., 2006, Planetary Space Sci, 52, 1399-1413, 2004a
21. Gopalswamy, N. (2000), Type II radio bursts, in Radio Astronomy at Long Wavelengths, Geophys. Monogr. Ser., vol. 119, edited by R. G. Stone etal., p. 123, AGU, Washington, D. C.
22. Gopalswamy et al. 2001, Journal of Geophysical Research, Volume 106, Issue A12, p. 29219-29230
23. Gopalswamy et al. 2009a; Gopalswamy, et al., Sol. Phys., 259, 227–254
24. Guhathakurta, M.; Fisher, R.; Strong, K.,1998; Observational Plasma Astrophysics : Five Years of Yohkoh and Beyond. Edited by Tetsuya Watanabe, Kluwer Academic Publishers, v. 229., p.13
25. Kosugi, T., 1971, Solar Phys., 48, 339 – 356.
26. Lara, A., Gopalswamy, N. Nunes, S., Munoz, G., & Yashiro, S. 2003, Geophys. Res. Lett., 30(12), 8016 27. Leblanc, Y., Dulk, G. A., Vourlidas, A., & Bougeret, J.-L. 2001,J. Geophys. Res., 160, 25,301
28. Lin, 2002,In: Solar variability: from core to outer frontiers. Ed. A. Wilson. ESA SP-506, Vol. 2. Noordwijk: ESA Publications Division, ISBN 92- 9092-816-6, 1035 – 1044
29. Liu, Y., Luhmann, J.G., Bale, S.D., Lin, R.D.: 2009, Astrophys. J. Lett. 691, L151.
30. Magdalenic et al, 2010,The Astrophysical Journal, Volume 718, Issue 1, pp. 266-278
31. Magdalenic et al , 2012,The Astrophysical Journal, Volume 746, Issue 2, article id. 152, 8 pp
32. Magdalenic et al,2008, Solar Physics, Volume 253, Issue 1-2, pp. 305-317
33. Maia, D., Pick, M., Vourlidas, A., & Howard, R. 2000, ApJ, 528, L49
34. Mancuso, S., et al, Astronomy and Astrophysics, Volume 463, Issue 3, March I 2007, pp.1137-114133.
35. Mann, G. 1995, J. Plasma Phys., 53, 109
36. Mann, G., et al,2007, The High Energy Solar Corona: Waves, Eruptions, Particles, Lecture Notes in Physics, Volume 725. Springer-Verlag Berlin Heidelberg, p. 203
37. Moses, D., Clette, F., Delaboudinière, J.P., Artzner, G.E., et al.: 1997, Solar Phys. 175, 571 – 599.
38. Miteva, Mann, 2007, Astronomy and Astrophysics, Volume 474, Issue 2, November I 2007, pp.617-625
39. Nelson, G. J. and Robinson R. D.: 1975, Proc. Astron. Soc. Aust. 2, 370.
40. Nelson, G.J., and Melrose, D.B., in Solar Radio Physics, edited by D.J.McLean and R.D.Robinson, Cambridge, Newyork, p 333, 1985.
41. Newkirk, G. A.: 1961, Astrophys. J. 133, 983.
42. Nindos,A.;Alissandrakis,C.E.;Hillaris,A.;Preka-Papadema,P.,2011, Astronomy & Astrophysics, Volume 531, id.A31, 12 pp
43. Parenti,s.: et al, 2000, Astronomy and Astrophysics, v.363, p.800-814
44. Pick, M., & Vilmer, N. 2008, A&AR, 16, 1
45. Prakash et al. 2010, Solar Physics, Volume 266, Issue 1, pp.135-147
46. Ramesh et al. 2010, The Astrophysical Journal, Volume 712, Issue 1, pp. 188-193
47. Reiner, M. J., Kaiser, M. L., Gopalswamy, N., Aurass, H., Mann, G., Vourlidas, A., Maksimovic, M., 2001a. J. Geophys Res. 106, 25279-25290
48. Reiner, M. J., M. L. Kaiser, and J. L. Bougeret , 2001b, J. Geophys. Res., 106, 29,989.
49. Saito, K., Poland, A. I., & Munro, R. H. 1977, Sol. Phys. 55, 121
50. Schwartz, et al, 2011, Physical Review Letters, vol. 107, Issue 21, id. 215002
51. Sckopke, N.1995, Advances in Space Research (ISSN 0273-1177), vol. 15, no. 8-9, p. 261-269
52. Stewart, R. T., M. McCabe, M. J. Koomen, R. T. Hansen, G. A. Dulk, Solar Phys., 36, 203, 1974a
53. Stewart, R. T., R. A. Howard, F. Hansen, T. Gergely, M. Kundu, Solar Phys., 36, 219, 1974b
54. Subramanian & E.Ebenezer, 2006,A&A,683,451
55. Thompson, B.J., Plunkett, S.P., Gurman, J.B., Newmark, J.S., St. Cyr, O.C., and Michels, D.J.: 1998, Geophys. Res. Lett. 25, 2465.
56. Thomsen ey al, 1985, Journal of Geophysical Research (ISSN 0148-0227), 90, 137-148
57. Vršnak, B., Cliver, E.: 2008, Solar Phys. 253, 215.
58. Vr˘snak, B., Aurass, H., Magdaleni´c, J., & Gopalswamy, N. 2001,A&A, 377, 321
59. Wagner, W. J. & MacQueen, R. M., 1983, A&A, 120, 136
60. Wild, J.P., and McReady, L.L. 1950, Aust.J. Sci.Res, A3, 387
61. Zhang, M., & Low, B. C. 2001, ApJ, 561, 406
62. Zheleznyakov, V. V.: 1970, Radio Emission of the Sun and the Planets. Oxford: Pergamon Press Ltd.